

Greybody Factor for a Static Spherically Symmetric Black Hole With Non-Linear Electrodynamics

M. Sharif ^{*} and A. Raza [†]

Department of Mathematics, University of the Punjab,
Quaid-e-Azam Campus, Lahore-54590, Pakistan.

Abstract

In this paper, we study the greybody factor for static spherically symmetric black hole with non-linear electrodynamics. For this purpose, we assume minimal coupling of the scalar field and find the radial equation by using the Klein-Gordon equation. We then apply tortoise coordinate to convert this equation into Schrodinger wave equation which helps to find the effective potential. The behavior of effective potential is checked for different values of the coupling and charge parameters. We find two solutions in two horizons named as event and cosmological horizons by using the radial equation. We consider the intermediate regime and match these two solutions to obtain the greybody factor and examine its behavior graphically. It is found that the greybody factor has an inverse relation with the coupling constant, mass, charge as well as the radius of the black hole and has a direct relation with angular momentum.

Keywords: Greybody factor; Black hole; Hawking radiation; Electrodynamics; Effective potential.

PACS: 04.70.-s; 04.70.Dy.

^{*}msharif.math@pu.edu.pk

[†]aliraza008.math@gmail.com

1 Introduction

Black holes (BHs) are some of the strangest and most fascinating objects in outer space. They are extremely dense, with such strong gravitational attraction that even light cannot escape their grasp if it comes near enough. Some well-known BHs are developed by Schwarzschild, Reissner-Nordstrom, Kerr and Kerr-Newman based on the physical parameters. Singularity is the most crucial issue in gravitational physics as it is a point in spacetime where physical laws break down. Bardeen [1] was the pioneer in the study of non-singular BH solutions, known as regular BHs. Kiselev [2] proposed the solutions of Schwarzschild BH surrounded by the quintessence matter in the presence and absence of charge. Hayward [3] extended the Bardeen concept and considered the BH with a non-singular static region of trapped surfaces.

Many BH solutions were developed for the quintessence field by using the Kiselev algorithm. Chen and Jing [4] calculated the frequencies of the massless scalar field around static spherically symmetric BHs. Bambi and Modesto [5] applied the Newman-Janis algorithm to Bardeen as well as Hayward BHs and obtained a family of rotating non-singular solutions for both metrics. Xu et al [6] found a spherically symmetric BH solution by using Newman-Janis technique and obtained a relation between perfect fluid dark matter and the cosmological constant. They also extended this solution for the de Sitter and anti-de Sitter spacetimes. Xu et al [7] generalized Reissner-Nordstrom BH to the Kerr-Newman-anti-de Sitter BH and examined that there is no effect of perfect fluid dark matter on singularity.

The laws of thermodynamics such as the law of conservation of energy and the law of entropy (the entropy of an isolated system always increases) also hold in BH thermodynamics. This idea attracted Hawking and proposed that if BH has temperature then it must emit some radiations called Hawking radiations [8]. The rate at which it emits radiations is defined as

$$\gamma(w) = \left(\frac{d^3k}{(e^{\frac{w}{t_h}} \pm 1)8\pi^3} \right),$$

where t_h , w and k are the Hawking temperature, frequency and surface gravity, respectively. Here d shows the change in surface gravity from k to δk . Since the emission rate has an inverse relation to the size of BH, therefore, smaller BHs will emit radiations faster than the larger BHs. The above expression can be generalized for any dimension as well as massive and non-massive particles. The positive and negative signs show boson and fermion

particles, respectively. Hawking radiations give information about the physical features inside the BH such as charge, angular momentum, mass, etc.

The exterior region of a BH plays the role of potential barrier for radiations, thus the spectrum formed at the event horizon is similar to the black-body spectrum. The potential required for Hawking radiations to cross the curvature outside the event horizon of BH is called effective potential. However, Hawking radiations cannot cross the barrier completely, therefore, the observer cannot observe the same spectrum of these radiations. Consequently, an observer outside the event horizon will observe the emission rate differently from the real one. Thus, the emission rate for the observer is expressed as

$$\gamma(w) = \left(\frac{|G_{M,l}|^2 d^3k}{(e^{\frac{w}{\hbar}} \pm 1) 8\pi^3} \right),$$

where $|G_{M,l}|^2$ is a greybody factor (GF) based on the frequency. The GF is the probability of waves arriving from infinity and absorbed by BH [9]-[12]. This factor is more significant as it changes the Hawking radiation formula and is used to calculate the absorption cross-section of BH. It is observed that Hawking temperature and entropy vary with respect to the size of BHs [13]-[15].

Ida et al [16] used the scalar field in higher dimensions to examine the GF of rotating BH in a low-frequency expansion. Creek et al [17] investigated the GF for Bardeen BH and checked the emission rate of the scalar field by analytical and numerical methods. Chen et al [18] calculated the GF for d-dimensional BH by using quintessence field and obtained that frequency increases as the luminosity of radiation decreases. They also found that the corresponding solutions reduce to the d-dimensional Reissner-Nordstrom BH for the specific value of frequency. Crispino et al [19] investigated the absorption process of Schwarzschild BH for non-minimally coupled scalar fields. Kanti et al [20] derived the GF for the scalar field by using higher-dimensional Schwarzschild-de Sitter spacetime.

Jorge et al [21] computed the GF for higher-dimensional rotating BHs with the cosmological constant in a low-frequency regime. Toshmatov et al [22] measured the effect of charge as well as absorption rate for regular BHs and found that charge reduces the transmission factor for incident waves. Ahmad and Saifullah [23] used cylindrically symmetric spacetime and found GF for the uncharged and massless scalar field. Dey and Chakrabarti [24] considered Bardeen-de Sitter spacetime and measured the probability of ab-

sorption as well as quasinormal modes. Sharif and Ama-Tul-Mughani [25] examined the GF for rotating Bardeen and Kerr-Newman BHs surrounded by quintessence. In a recent paper [26], Sharif and Shaukat calculated the GF for a rotating Bardeen BH surrounded by perfect fluid dark matter.

Born and Infeld [27] used non-linear electrodynamics (NLED) to ensure that the self-energy of a point-like charge is finite. Beato and Garcia [28] coupled general relativity with NLED to find a non-singular BH solution. Cai et al [29] coupled BHs with Born-Infeld NLED and found the importance of the cosmological constant in the stable region of BH. The static spherically symmetric BH with NLED, minimally/non-minimally coupled with gravity has become a subject of great interest for the researchers. Bolokhov et al [30] developed examples of minimally coupled BHs with gravity having four different horizons. The non-minimally coupled BHs with gravity are important for dark energy and inflation. Many singular as well as non-singular BHs with NLED have been constructed in [31]. No hair conjecture states that BH is described completely by only three parameters like mass, charge and spin. Chowdhury and Banerjee [32] evaluated GF for Reissner-Nordstrom BH endowed with a scalar hair and gave the counter-example of no hair conjecture. They observed the opposite behavior of hairy scalar as compared to charge parameter.

This paper explores the effective potential and GF for static spherically symmetric BH with NLED. The paper is planned as follows. In section 2, we find the effective potential by using the radial equation of motion and tortoise coordinate. We find solutions of the radial equation near and far away from the horizons in section 3. Section 4 matches the obtained solutions in the intermediate regime and finds GF. The summary of the results is given in section 5.

2 Effective Potential

In this section, we formulate the effective potential required for Hawking radiations. We consider a static spherically symmetric BH with NLED as [33]

$$ds^2 = -h(r)dt^2 + \frac{dr^2}{h(r)} + r^2(d\theta^2 + \sin^2\theta d\phi^2), \quad (1)$$

where

$$h(r) = 1 - \frac{2M}{r} + \frac{Q^2}{r^2} - \frac{r^2\alpha^2}{3} + 2\alpha Q. \quad (2)$$

Here, α is a coupling constant while Q and M represent charge and mass of the BH, respectively. It is mentioned here that Schwarzschild BH is recovered for $Q = \alpha = 0$. To find the roots of Eq.(2), we take $h(r) = 0$, which yields

$$1 - \frac{2M}{r} + \frac{Q^2}{r^2} - \frac{r^2\alpha^2}{3} + 2\alpha Q = 0. \quad (3)$$

Its solution gives two horizons as event horizon (near to BH) and cosmological horizon (far away from BH). In order to analyze the propagation of scalar field, we assume that particles and gravity are minimally coupled and use the Klein-Gorden equation as

$$\partial_\delta[\sqrt{-g}g^{\delta\nu}\partial_\nu\Sigma] = 0. \quad (4)$$

This equation is solved by using separation of variables method as

$$\Sigma = \exp(-\iota wt)R_{wlm}(r)Y_m^l(\theta, \phi),$$

where $Y_m^l(\theta, \phi)$ shows angular behavior. Thus, Eq.(4) turns out to be

$$\frac{1}{r^2} \left(r^2 h \frac{d}{dr} R_{wlm} \right)_{,r} + \left(\frac{w^2}{h} - \frac{\lambda_l}{r^2} \right) R_{wlm} = 0, \quad (5)$$

$$\frac{1}{\sin\theta} \left(\sin\theta \frac{\partial Y_m^l}{\partial\theta} \right)_{,\theta} + \frac{1}{\sin^2\theta} \frac{(\partial^2 Y_m^l)}{\partial\phi^2} + \lambda_l Y_m^l = 0, \quad (6)$$

where λ_l is a separation constant. This determines the connection between radial and angular equations [34]. The power series of separation constant is given by [35]

$$\lambda_l = \sum_{k=0}^{\infty} (aw)^k F_k^{lm}, \quad \lambda_l = l(l+1) + O(s, w). \quad (7)$$

Here, orbital angular momentum (l) satisfies the conditions $l \geq |m|$ and $\frac{l-|m|}{2} \in (0, \mathbb{Z})$, \mathbb{Z} represents the set of integers. First, we find the potential which affects the outgoing radiation from the BH. For this purpose, we

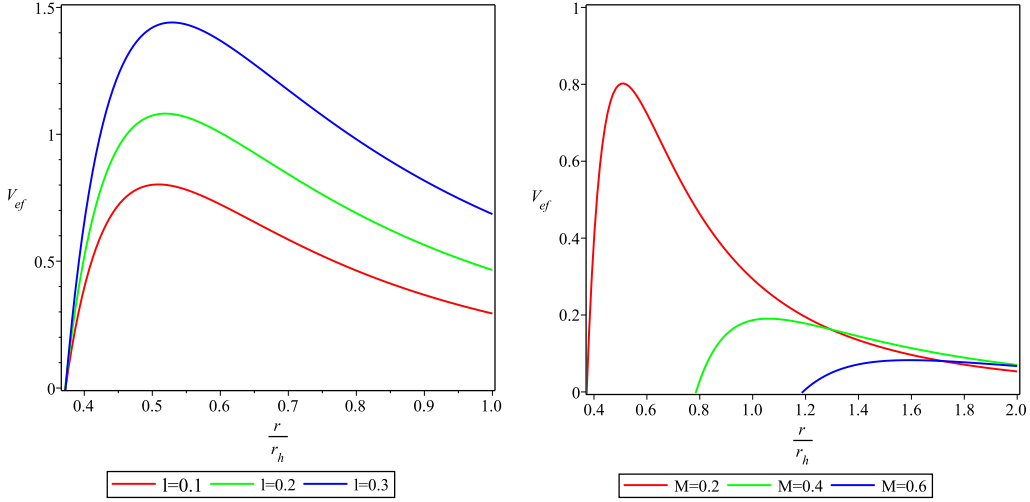


Figure 1: Plots of effective potential versus $\frac{r}{r_h}$ with $M = 0.2$ (left) and with $l = 0.1$ (right) for $Q = 0.1$, $\alpha = 0.01$ and $w = 0.1$.

redefine the radial equation and introduce a new coordinate called tortoise coordinate (v_*) as

$$R_{wlm}(r) = \frac{T_{wlm}(r)}{r}, \quad \frac{dv_*}{dr} = \frac{1}{h}, \quad \frac{d}{dv_*} = h \frac{d}{dr}, \quad \frac{d^2}{dv_*^2} = h \left(\frac{d^2}{dr^2} + \frac{dh}{dr} \frac{d}{dr} \right).$$

We can observe that $r \rightarrow r_h \Rightarrow v_* \rightarrow -\infty$ and $r \rightarrow \infty \Rightarrow v_* \rightarrow \infty$. The radial equation works for both (inside/outside) event horizons. The corresponding radial equation becomes

$$\left(\frac{d^2}{dv_*^2} - V_{ef} \right) T_{wlm} = 0, \quad (8)$$

where $V_{ef} = h \left(\frac{1}{r} \frac{dh}{dr} - w^2 + \frac{\lambda_l}{r^2} \right)$ is the effective potential which vanishes at $h = 0$. We can analyze its behavior through graphs for different physical parameters.

The behavior of effective potential for various values of mass and angular momentum is given in Figure 1. The graph in the right panel shows that the height of effective potential is higher for the smaller value of mass corresponding to the radial coordinate. The angular momentum in the left graph has a direct relation with the effective potential which minimizes the GF. In

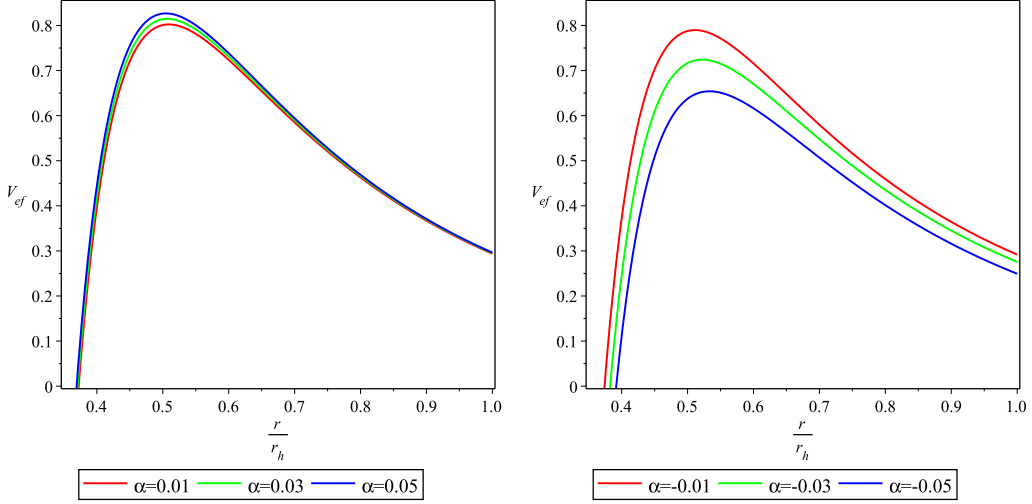


Figure 2: Plots of effective potential versus $\frac{r}{r_h}$ with $\alpha > 0$ (left) and $\alpha < 0$ (right) for $M = 0.2$, $Q = 0.1$ and $w = 0.1$.

Figure 2, the behavior of the effective potential shows direct relation with the coupling constant that lowers the emission rate. Figure 3 (left plot) shows that the effective potential decreases with the increase of charge parameter. This behavior shows that the presence of charge parameter decreases the effective potential which increases the absorption probability. The right graph shows that the effective potential decreases with the frequency of Hawking radiations which indicates the increasing behavior of the GF.

3 Greybody Factor

This section evaluates the GF by analytical approach. We use radial equation and apply transformations near and far away from the event horizon. We then match both solutions in the middle region. These transformations give suitable equations which can be solved analytically. The first transformation near the horizon is

$$r \rightarrow \Theta = \frac{1 - \frac{2M}{r} + \frac{Q^2}{r^2} - \frac{r^2\alpha^2}{3} + 2\alpha Q}{1 - \frac{r^2\alpha^2}{3}}, \quad \frac{d\Theta}{dr} = \frac{(1 - \Theta)P}{r(3 - r^2\alpha^2)}, \quad (9)$$

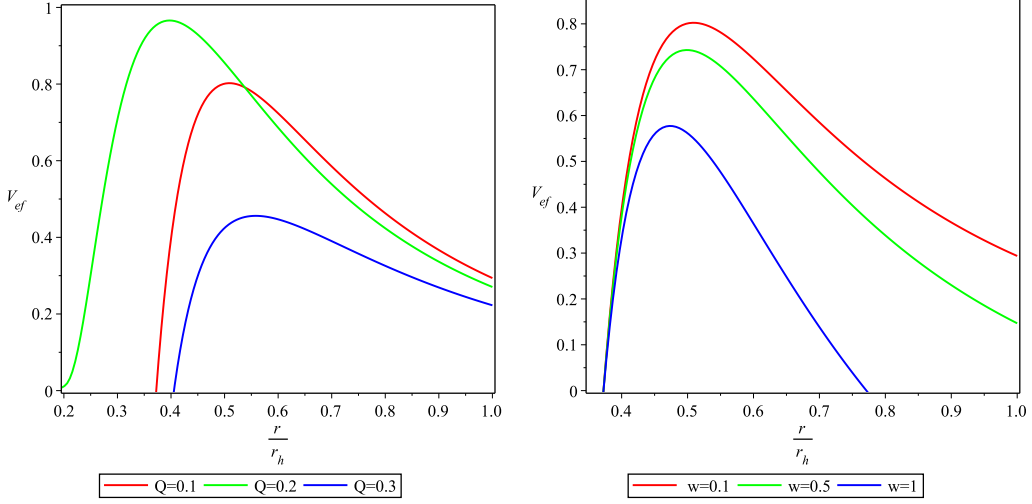


Figure 3: Plots of effective potential versus $\frac{r}{r_h}$ with $w = 0.1$ (left) and $Q = 0.1$ (right) for $l = 0.1$, $M = 0.2$, $l = 0.1$ and $\alpha = 0.01$.

where

$$P = \frac{2(3Mr + 3Q^2 - (3Mr + 2Q^2)\alpha^2 r^2 - 2\alpha^3 Q r^4)}{2Mr - Q^2 - 2Q\alpha r^2}.$$

Using Eq.(9) in the radial equation, we have

$$\Theta(1 - \Theta) \frac{d^2 R_{wlm}}{d\Theta^2} + (B - A\Theta) \frac{dR_{wlm}}{d\Theta} + \frac{1}{(1 - \Theta)P^2} (\zeta_h - \xi_h) R_{wlm} = 0, \quad (10)$$

where

$$A = \frac{3(rh(1 - \Theta)P)'}{(1 - \Theta)P^2}, \quad B = -\frac{2r^2\alpha^2}{P}, \quad \zeta_h = 9w^2r^2, \quad \xi_h = 3(l^2 - l)(3 - r^2\alpha^2).$$

We use the transformation ($R_{wlm}(\Theta) = \Theta^{\pi_1}(1 - \Theta)^{\tau_1}W_{wlm}(\Theta)$) in Eq.(10) to obtain hypergeometric (HG) equation. The corresponding equation becomes

$$\begin{aligned} & \Theta(1 - \Theta) \frac{d^2 W_{wlm}}{d\Theta^2} + [2\pi_1 + B - (2\pi_1 + 2\tau_1 + A)\Theta] \frac{dW_{wlm}}{d\Theta} + \left[\frac{1}{\Theta}(\pi_1^2 - \pi_1 \right. \\ & + B\pi_1 + \frac{\zeta_h}{P^2}) + \frac{1}{1 - \Theta}(\tau_1^2 - \tau_1 - B\tau_1 + A\tau_1 + \frac{\zeta_h}{P^2} - \frac{\xi_h}{P^2}) - (\tau_1 + \pi_1)A \\ & \left. - \pi_1^2 - 2\pi_1\tau_1 + \pi_1 - \tau_1^2 + \tau_1 \right] W_{wlm} = 0. \end{aligned}$$

In order to find the power coefficients, we assume that the coefficients of $\frac{1}{\Theta}$ and $\frac{1}{1-\Theta}$ are zero

$$\pi_1^2 - \pi_1(1 - B) + \frac{\zeta_h}{P^2} = 0, \quad \tau_1^2 - \tau_1(1 - A - B) + \frac{\zeta_h}{P^2} - \frac{\xi_h}{P^2} = 0.$$

The corresponding radial equation (5) turns out to be

$$\Theta(1 - \Theta) \frac{d^2 W_{wlm}}{d\Theta^2} + (k_1 - (i_1 + j_1 + 1)\Theta) \frac{dW_{wlm}}{d\Theta} - i_1 j_1 W_{wlm} = 0, \quad (11)$$

where $i_1 = \pi_1 + \tau_1$, $j_1 = \pi_1 + \tau_1 + A - 1$, $k_1 = 2\pi_1 + B$. The general solution of this equation for near the horizon is

$$(R_{wlm})_{nh}(\Theta) = I_1 \Theta^{\pi_1} (1 - \Theta)^{\tau_1} F(i_1, j_1, k_1; \Theta) + I_2 \Theta^{-\pi_1} (1 - \Theta)^{\tau_1} \\ \times F(1 - k_1 + i_1, 1 - k_1 + j_1, 2 - k_1; \Theta),$$

where I_1 and I_2 are constants and

$$\pi_1^\pm = \frac{1}{2} \left[(1 - B) \pm \sqrt{(1 - B^2) - 4 \frac{\zeta_h}{P^2}} \right], \\ \tau_1^\pm = \frac{1}{2} \left[(1 + B - A) \pm \sqrt{(1 - A + B)^2 + 4 \left(\frac{\xi_h}{P^2} \frac{\zeta_h}{P^2} \right)} \right].$$

Now, we apply the boundary conditions as outgoing wave is not observed near the event horizon. We can choose $I_1 = 0$, or $I_2 = 0$ depending upon whether π_1 is positive or negative. It is found that the choice of π_1 does not affect the choice of constants, therefore, we take $\pi_1 = \pi_1^-$ with $I_2 = 0$. The corresponding solution becomes

$$(R_{wlm})_{nh}(\Theta) = I_1 \Theta^{\pi_1} (1 - \Theta)^{\tau_1} F(i_1, j_1, k_1; \Theta). \quad (12)$$

Applying the same procedure for the cosmological horizon, we have

$$\Upsilon(r) = \frac{h}{r^2} = \frac{1}{r^2} - \frac{\alpha^2}{3}, \quad \frac{d\Upsilon}{dr} = \frac{(1 - \Upsilon)D}{r}, \quad (13)$$

where $D(r) = \frac{-6}{r^2(3+\alpha^2)-3}$. Using the transformation

$$R_{wlm}(\Upsilon) = \Upsilon^{\pi_2} (1 - \Upsilon)^{\tau_2} W_{wlm}(\Upsilon),$$

and Eq.(13) in (5), we obtain

$$\begin{aligned} & \Upsilon(1 - \Upsilon) \frac{d^2 W_{wlm}}{d\Upsilon^2} + (2\pi_2 + B_\star - (2\pi_2 + 2\tau_2 + A_\star)\Upsilon) \frac{dW_{wlm}}{d\Upsilon} \\ & + \left[(\pi_2^2 - \pi_2 + B_\star\pi_2 + \frac{\zeta_\star}{D^2}) \frac{1}{\Upsilon} + (\tau_2^2 - \tau_2 - B_\star\tau_2 + A_\star\tau_2 + \frac{\zeta_\star}{D^2} - \frac{\xi_\star}{D^2}) \right. \\ & \left. \times \frac{1}{1 - \Upsilon} - \pi_2^2 - 2\pi_2\tau_2 - A_\star(\pi_2 - \tau_2 + \pi_2 + \tau_2) \right] W_{wlm} = 0. \end{aligned}$$

To find the power coefficients π_2 and τ_2 , we assume the coefficients of $\frac{1}{\Upsilon}$ and $\frac{1}{1-\Upsilon}$ to be zero

$$\pi_2^2 - \pi_2(1 - B_\star) + \frac{\zeta_\star}{D^2} = 0, \quad \tau_2^2 - \tau_2(1 - A_\star - B_\star) + \frac{\zeta_\star}{D^2} - \frac{\xi_\star}{D^2} = 0.$$

The corresponding radial equation in the form of HG equation turns out to be

$$\Upsilon(1 - \Upsilon) \frac{d^2 W_{wlm}}{d\Upsilon^2} + (k_2 - (i_2 + j_2 + 1)\Upsilon) \frac{dW_{wlm}}{d\Upsilon} - i_2 j_2 W_{wlm} = 0, \quad (14)$$

where $i_2 = \pi_2 + \tau_2$, $j_2 = \pi_2 + \tau_2 + A_\star - 1$, $k_2 = 2\pi_2 + B_\star$. The general solution of HG equation is

$$\begin{aligned} (R_{wlm})_{fh}(\Upsilon) &= J_1 \Upsilon^{\pi_2} (1 - \Upsilon)^{\tau_2} F(i_2, j_2, k_2; \Upsilon) + J_2 \Upsilon^{\pi_2} (1 - \Upsilon)^{\tau_2} \\ &\times F(1 + i_2 - k_2, 1 + j_2 - k_2, 2 - k_2; \Upsilon), \end{aligned} \quad (15)$$

where J_1 and J_2 are arbitrary constants.

4 Matching Regime

Here, we match the obtained solutions at the event and cosmological horizons in the intermediate region corresponding to r . For this reason, we stretch the event horizon towards the cosmological horizon by replacing the argument Θ by $1 - \Theta$ of HG function in Eq.(12) and obtain

$$\begin{aligned} (R_{wlm})_{nh}(\Theta) &= I_1 \Theta^{\pi_1} (1 - \Theta)^{\tau_1} \left[\frac{\Gamma(-i_1 - j_1 + k_1) \Gamma(k_1)}{\Gamma(k_1 - i_1) \Gamma(k_1 - j_1)} F(i_1, j_1, k_1; 1 - \Theta) \right. \\ &+ (1 - \Theta)^{-i_1 - j_1 + k_1} \frac{\Gamma(k_1) \Gamma(i_1 + j_1 - k_1)}{\Gamma(j_1) \Gamma(i_1)} \\ &\left. \times F(k_1 - i_1, k_1 - j_1, 1 - i_1 - j_1 + k_1; 1 - \Theta) \right]. \end{aligned}$$

Using Eqs.(3) and (9), we have

$$1 - \Theta = \frac{3(2Mr - Q^2 - 2Qr^2\alpha)}{r^2(3 - r^2\alpha^2)}.$$

The extended event horizon for $\Theta \rightarrow 1$ and $r \gg r_h$ is

$$(1 - \Theta)^{\tau_1} \simeq (Q_\star^2 + 2\alpha Q)^{\tau_1} \left(\frac{r}{r_h}\right)^{\tau_1} \Rightarrow (1 - \Theta)^{\tau_1} \simeq (Q_\star^2 + 2\alpha Q)^{-l} \left(\frac{r}{r_h}\right)^{-l},$$

and

$$\begin{aligned} (1 - \Theta)^{\tau_1 + k_1 - i_1 - j_1} &\simeq (Q_\star^2 + 2\alpha Q)^{-\tau_1 + B - A + 1} \left(\frac{r}{r_h}\right)^{-\tau_1 + B - A + 1} \\ &\simeq (Q_\star^2 + 2\alpha Q)^{l+1} \left(\frac{r}{r_h}\right)^{l+1}, \end{aligned}$$

where $Q_\star = \frac{Q}{r_h}$. It is worthwhile to mention here that the constraints are valid for small values of charge and coupling parameters. In an intermediate zone, both parts of near horizon BH solution can be written as

$$(1 - \Theta)^{\tau_1} \simeq (Q_\star^2 + 2\alpha Q)^l \left(\frac{r}{r_h}\right)^{-l}, \quad (1 - \Theta)^{\tau_1} \simeq (Q_\star^2 + 2\alpha Q)^{1+l} \left(\frac{r}{r_h}\right)^{1+l}.$$

Finally, the solution on the event horizon is

$$(R_{wlm})_{nh}(\Theta) = I' \left(\frac{r}{r_h}\right)^{-l} + I_2' \left(\frac{r}{r_h}\right)^{l+1}, \quad (16)$$

with

$$\begin{aligned} I_1' &= I_1 (Q_\star^2 + 2\alpha Q)^{-l} \frac{\Gamma(-i_1 - j_1 + k_1) \Gamma(k_1)}{\Gamma(k_1 - i_1) \Gamma(k_1 - j_1)}, \\ I_2' &= (Q_\star^2 + 2\alpha Q)^{l+1} \frac{\Gamma(k_1) \Gamma(i_1 + j_1 - k_1)}{\Gamma(j_1) \Gamma(i_1)}. \end{aligned}$$

Now, we shift the cosmological horizon to the event horizon. Therefore, we replace the argument Υ by $1 - \Upsilon$ of HG function in Eq.(15) and obtain

$$\begin{aligned} (R_{wlm})_{fh}(\Upsilon) &= J_1 \Upsilon^{\pi_2} (1 - \Upsilon)^{\tau_2} \left[\frac{\Gamma(-i_2 - j_1 + k_1) \Gamma(k_2)}{\Gamma(k_2 - i_2) \Gamma(k_2 - j_2)} F(i_2, j_2, k_2; 1 - \Upsilon) \right. \\ &+ F(k_2 - i_2, k_2 - j_2, 1 - i_2 - j_2 + k_2; 1 - \Upsilon) \frac{\Gamma(k_2) \Gamma(i_2 + j_2 - k_2)}{\Gamma(j_2) \Gamma(i_2)} \\ &\left. \times (1 - \Upsilon)^{-i_2 - j_2 + k_2} \right] + J_2 \Theta^{-\pi_2} (1 - \Upsilon)^{\tau_2} \left[\frac{\Gamma(-i_2 - j_2 + k_2) \Gamma(2 - k_2)}{\Gamma(1 - i_2) \Gamma(1 - j_2)} \right. \\ &\times F(-k_2 + i_2 + 1, j_2 - k_2 + 1, 2 - k_2; 1 - \Upsilon) + (1 - \Theta)^{-i_2 - j_2 + k_2} \\ &\left. \times \frac{\Gamma(2 - k_2) \Gamma(i_2 + j_2 - k_2)}{\Gamma(1 - i_2) \Gamma(1 - j_2)} F(1 - i_2, 1 - j_2, 1 - i_2 - j_2 + k_2; 1 - \Upsilon) \right]. \quad (17) \end{aligned}$$

To find the solution of cosmological horizon, we consider $\Upsilon(r_f) \rightarrow 0$, so that the corresponding Eq.(13) becomes

$$1 - \Upsilon = \frac{r}{r_f} \left(\frac{1}{rr_f} - \frac{r_f}{r^3} + \frac{r_f}{r} \right). \quad (18)$$

This equation can be written in the following form

$$(1 - \Upsilon)^{\tau_2} \simeq \left(\frac{r}{r_f} \right)^{-l} \left(\frac{1}{rr_f} - \frac{r_f}{r^3} + \frac{r_f}{r} \right)^{-l},$$

and

$$(1 - \Upsilon)^{\tau_2 - i_2 - j_2 + k_2} \simeq \left(\frac{r}{r_f} \right)^{l+1} \left(\frac{1}{rr_f} - \frac{r_f}{r^3} + \frac{r_f}{r} \right)^{l+1}.$$

The corresponding Eq.(17) turns out to be

$$R_{fh} = (H'_1 J_1 + H'_2 J_2) \left(\frac{r}{r_f} \right)^{-l} + (H'_3 J_1 + H'_4 J_2) \left(\frac{r}{r_f} \right)^{l+1}, \quad (19)$$

where

$$\begin{aligned} H'_1 &= \frac{\Gamma(k_2)\Gamma(k_2 - i_2 - j_2)}{\Gamma(k_2 - i_2)\Gamma(k_2 - j_2)} \left(\frac{1}{rr_f} - \frac{r_f}{r^3} + \frac{r_f}{r} \right)^{-l}, \\ H'_2 &= \frac{\Gamma(2 - k_2)\Gamma(k_2 - i_2 - j_2)}{\Gamma(1 - i_2)\Gamma(1 - j_2)} \left(\frac{1}{rr_f} - \frac{r_f}{r^3} + \frac{r_f}{r} \right)^{-l}, \\ H'_3 &= \frac{\Gamma(k_2)\Gamma(-k_2 + i_2 + j_2)}{\Gamma(i_2)\Gamma(j_2)} \left(\frac{1}{rr_f} - \frac{r_f}{r^3} + \frac{r_f}{r} \right)^{l+1}, \\ H'_4 &= \frac{\Gamma(2 - k_2)\Gamma(-k_2 + i_2 + j_2)}{\Gamma(1 - i_2)\Gamma(1 - j_2)} \left(\frac{1}{rr_f} - \frac{r_f}{r^3} + \frac{r_f}{r} \right)^{l+1}. \end{aligned}$$

Comparing both the solutions, we obtain

$$I'_1 = H'_1 J_1 + H'_2 J_2, I'_2 = H'_3 J_1 + H'_4 J_2,$$

where

$$J_1 = \frac{I'_1 H'_4 - I'_2 H'_2}{H'_1 H'_4 - H'_2 H'_3}, \quad J_2 = \frac{I'_1 H'_3 - I'_2 H'_1}{H'_2 H'_3 - H'_1 H'_4}. \quad (20)$$

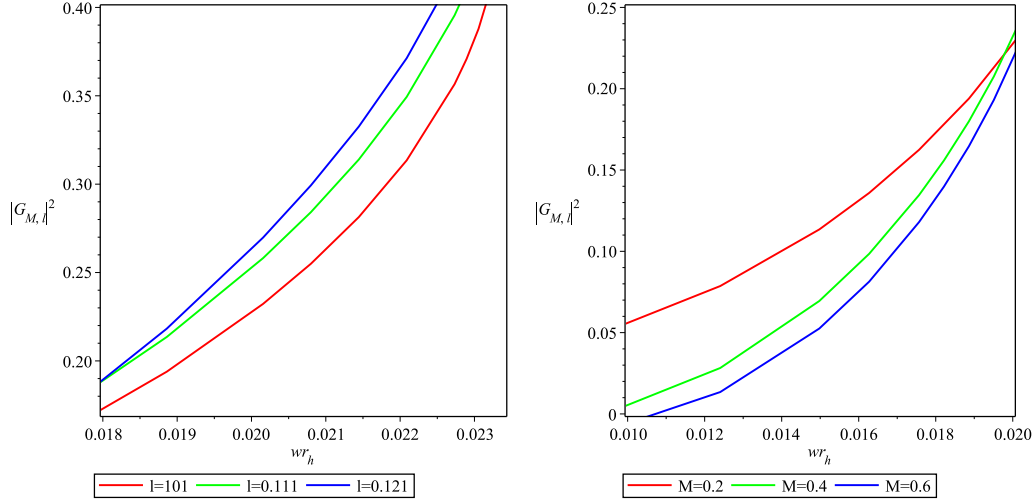


Figure 4: Plots of GF versus wr_h with $M = 0.2$ (left) and with $l = 0.101$ (right) for $r = 10.5$, $Q = 0.101$ and $\alpha = 0.05$.

Consequently, the expression for GF is given as

$$|G_{M,l}|^2 = 1 - \left| \frac{J_2}{J_1} \right|^2, \quad (21)$$

which takes the following form using Eq.(20)

$$|G_{M,l}|^2 = 1 - \left| \frac{I'_1 H'_3 - I'_2 H'_1}{I'_1 H'_4 - I'_2 H'_2} \right|^2.$$

This is the final expression of GF for the static spherically symmetric BH with NLED. It is observed that waves pass through the cosmological horizon which is far away from the event horizon. Then the waves either reflect or move forward implying that there is a connection between the frequency and the effective potential. It is noted that the waves must be of high frequency to cross the barrier easily.

We examine the effect of different physical parameters on GF through graphs. Figure 4 shows the relationship between mass and angular momentum, i.e., GF is smaller for higher values of mass and larger for greater values of the angular momentum. This indicates that GF decreases with the increase in the value of mass, and BH with a larger value of angular momentum has

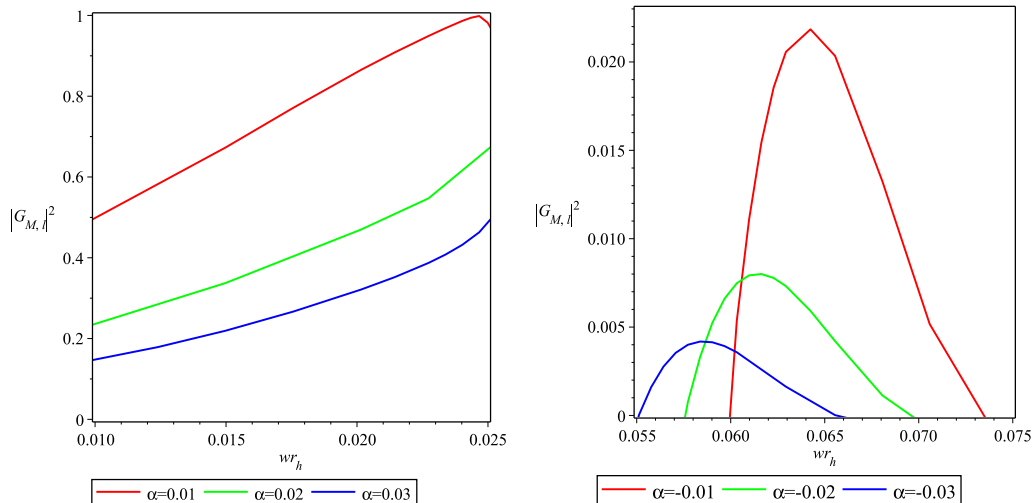


Figure 5: Plots of GF versus wr_h with $\alpha > 0$ (left) and with $\alpha < 0$ (right) for $M = 0.2$, $l = 0.101$, $r = 10.5$ and $Q = 0.101$.

a higher emission rate. Figures **5-6** indicate that GF decreases with the increase in the coupling and charge parameters. It shows that the presence of the coupling and charge parameters decreases the probability of absorption of the radiations. The GF has an inverse relation with radius and disappears after specific values of the radial coordinate. This indicates that BH with a larger size has a lower emission rate and the GF.

5 Conclusions

In this paper, we have analyzed the GF for static spherically symmetric BH with NLED. We have used the Klein-Gorden equation of motion and applied the separation of variables method to obtain the radial and angular equations. We have then used tortoise coordinate and transformed the radial equation into Schrodinger wave equation. Further, we have obtained the effective potential for the absorption of Hawking radiation and checked its behavior corresponding to the coupling, charge and frequency parameters graphically.

We have worked near the BH and cosmological horizons and transformed the radial equation into HG differential equations in both regions to obtain the solutions. In the intermediate regime, we have matched these two solu-

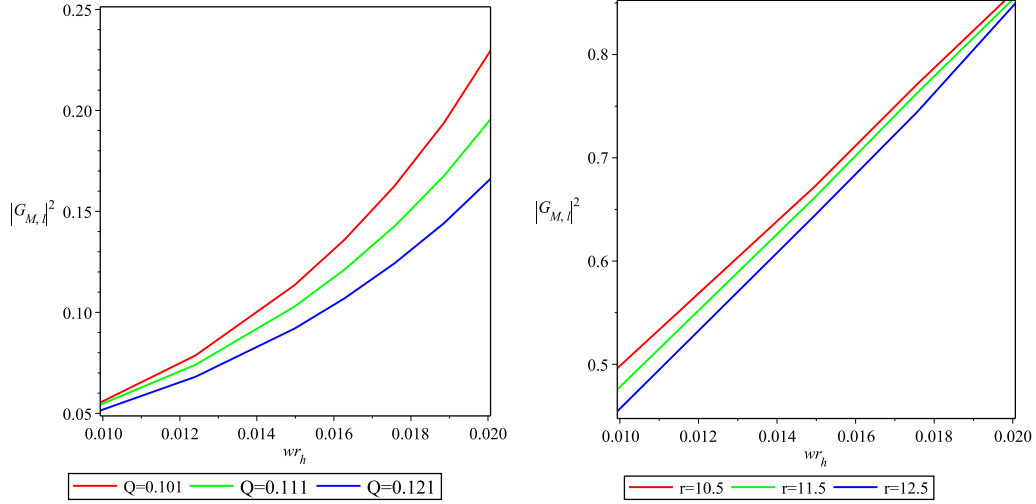


Figure 6: Plots of GF versus wr_h with $r = 10.5$ (left) and with $Q = 0.101$ (right) for $M = 0.2$, $l = 0.101$, and $\alpha = 0.05$.

tions by stretching the event horizon, compressing the cosmological horizon and have found the expression for GF. The main results of this paper are given as follows.

- We have found that the height of the effective potential (Figure 1) corresponding to radial parameter increases as the mass of BH decreases and angular momentum increases, consequently, the absorption probability reduces.
- The height of effective potential (Figures 2-3) decreases with a decrease in the coupling parameter and increases with an increase in charge and frequency parameters implying that the absorption probability decreases.
- It is found that the GF (Figure 4) corresponding to frequency parameter decreases as the mass of BH enhances which minimizes the emission rate. The GF increases for the higher value of angular momentum and vanishes at $l = 0$.
- We have found that the GF (Figures 5-6) has an inverse relation with coupling, charge and radial parameters.

The GF for static spherically symmetric BH with linear electrodynamics was studied in [36]. We have extended this work for NLED and discussed the effects of physical parameters on GF. The evaporation rate of a BH can be measured by using the GF as it is related to the emission of waves through the potential barrier. We have found that GF with NLED increases more rapidly as compared to linear electrodynamics. Thus, the presence of a non-linear charge increases the process of evaporation and can be expected for BH to die in a short span which is consistent with the literature [37]. It is worthwhile to mention here that our results reduce to Reissner-Nordstrom BH for $\alpha = 0$ and Schwarzschild BH for $\alpha = Q = 0$. It would be interesting to find GF for rotating spherically symmetric BH with NLED to reveal the influence of rotation on the GF.

References

- [1] Bardeen, J.M.: Proceedings of GR5 (Tiflis, USSR, 1968)174.
- [2] Kiselev, V.V.: Class. Quantum Grav. **20**(2003)1187.
- [3] Hayward, S.: Phys. Rev. Lett. **96**(2006)031103.
- [4] Chen, S. and Jing, J.: Class. Quantum Grav. **22**(2005)4651; **23**(2006)6141 ; Gen. Relativ. Gravit. **39**(2007)1003.
- [5] Bambi, C. and Modesto, L.: Phys. Lett. B **721**(2013)329.
- [6] Xu, Z., Hou, X. and Wang, J.: Class. Quantum Grav. **35**(2018)115003.
- [7] Xu, Z. et al.: Eur. Phys. J. C **78**(2018)513.
- [8] Hawking, S.W.: Nature **248**(1974)32; Commun. Math. Phys. **43**(1975)199.
- [9] Gubser, S.S. and Klebanov, I.R.: Phys. Rev. Lett. **77**(1996)4491.
- [10] Maldacena, J.M. and Strominger, A.: Phys. Rev. D **55**(1997)861.
- [11] Klebanov, I.R. and Mathur, S.D.: Nucl. Phys. B **500**(1997)115.
- [12] Kim, W.T. and John, J.: Phys. Lett. B **461**(1999)189.

- [13] Parikh, M.K. and Wilczek, F.: Phys. Rev. Lett. **85**(2000)5042.
- [14] Kerner, R. and Mann, R.B.: Class. Quantum Grav. **25**(2008)095014.
- [15] Ejaz, A. et al.: Phys. Lett. B **726**(2013)827.
- [16] Ida, D., Oda, K. and Park, S.C.: Phys. Rev. D **67**(2003)064025.
- [17] Creek, S. et al.: Phys. Lett. B **656**(2007)102.
- [18] Chen, S., Wang, B. and Su, R.: Phys. Rev. D **77**(2008)124011.
- [19] Crispino, L.C.B. et al.: Phys. Rev. D **87**(2013)104034.
- [20] Kanti, P., Pappas, T. and Pappas, N.: Phys. Rev. D **90**(2014)124077.
- [21] Jorge, R., de Oliveira, E.S. and Rocha, J.V.: Class. Quantum Grav. **32**(2015)065008.
- [22] Toshmatov, B. et al.: Phys. Rev. D **91**(2015)083008.
- [23] Ahmad, J. and Saifullah, K.: Eur. Phys. J. C **77**(2017)885.
- [24] Dey, S. and Chakrabarti, S.: Eur. Phys. J. C **79**(2019)504.
- [25] Sharif, M. and Ama-Tul-Mughani, Q.: Eur. Phys. J. Plus **134**(2019)616;
Phys. Dark Universe **27**(2020)100436.
- [26] Sharif, M. and Shaukat, S.: Ann. Phys. **436**(2021)168673.
- [27] Born, M. and Infeld, L.: Proc. Roy. Soc. Lond. A **143**(1934)410;
144(1934)425.
- [28] Beato, A.E. and Garcia, A.: Phys. Lett. B **464**(1999)25.
- [29] Cai, R.G., Pang D.W. and Wang, A.: Phys. Rev. D **70**(2004)124034.
- [30] Bolokhov, S.V., Bronnikov, K.A. and Skvortsova, M.V.: Class. Quantum Grav. **29**(2012)245006.
- [31] Beonnikove, K.A., Dymnikova, I.G. and Galaktinov, E.: Class. Quantum Grav. **29**(2012)095025; Yu, S. and Gao, C.: Int. J. Mod. Phys. A **29**(2019)2050032.

- [32] Chowdhury, A. and Banerjee, N.: Phys. Lett. B **805**(2020)135417.
- [33] Yu, S. and Gao, C.: Int. J. Mod. Phys. D **29**(2020)2050032.
- [34] Flammer, C.: *Spheroidal Wave Functions* (Stanford University Press, 1957).
- [35] Berti, E., Cardoso, V. and Casals, M.: Phys. Rev. D **73**(2006)024013; ibid. 109902.
- [36] Boonserm, P., Ngampitipan, T. and Wongjun, P.: Eur. Phys. J. C **78**(2018)492.
- [37] Okyay, M. and Övgün, A.: J. Cosmol. Astropart. Phys. **2022**(2022)009.